Biological Journal of the Linnean Society, 2003, **78**, 173–191. With 6 figures

The tooth of perfection: functional and spatial constraints on mammalian tooth shape

ALISTAIR R. EVANS* and GORDON D. SANSON

School of Biological Sciences, Clayton Campus, PO Box 18, Monash University, Victoria 3800, Australia

Received 22 April 2002; accepted for publication 19 September 2002

This paper addresses the question of how close mammalian teeth are to ideal functional forms. An 'ideal' form is a morphology predicted to be the best functional shape according to information of the relationships between shape and function. Deviations from an ideal form are likely to indicate the presence of developmental or genetic constraints on form. Model tools were constructed to conform to functional principles from engineering and dental studies. The final model shapes are very similar to several mammalian tooth forms (carnassial teeth and tribosphenic-like cusps), suggesting that these tooth forms very closely approach ideal functional forms. Further evidence that these tooth forms are close to ideal comes from the conservation over 140 million years, the independent derivation and/or the occurrence over a size range of several orders of magnitude of these basic tooth forms. One of the main functional shapes derived here is the 'protoconoid', a fundamental design for double-bladed tools that fits a large number of functional parameters. This shape occurs in tooth forms such as tribosphenic, dilambdodont and zalambdodont. This study extends our understanding of constraints on tooth shape in terms of geometry (how space influences tooth shape) and function (how teeth divide food). *Biological Journal of the Linnean Society*, 2003, **78**, 173–191.

ADDITIONAL KEYWORDS: dentition – functional morphology – tooth modelling – carnassial – protoconoid – VRML reconstruction.

INTRODUCTION

At times, biological form appears to have reached perfection. Enzymes that act as perfect catalysts are found in a very wide range of organisms (where the reaction rate of such enzymes is limited by the diffusion of substrate molecules; Knowles & Albery, 1977). However, we presume that in the majority of cases, morphology does not achieve perfection due to the myriad constraints imposed on its form. Constraints have been generally grouped as formal, historical or functional (Gould, 1989). Formal refers to constraints due to geometry and the principles of physics, for example, only a limited number of physical shapes are permitted in the confines of three-dimensional space (Thompson, 1942; Stevens, 1974). Historical constraints embody the results of the particular consequences of a taxon's history, and so such constraints are usually taxon-specific (Maynard Smith *et al*., 1985). 'Developmental' constraints can be considered the expression of historical and formal constraints through ontogeny (Gould, 1989). Functional demands placed on morphology will also constrain shape. These can arise from many sources, and can often be in conflict (e.g. the inability to maximize both mechanical advantage of jaw muscles and gape; Lessa & Stein, 1992).

Mammalian dentition is an interesting sphere in which to investigate perfection and the influence of constraints on morphology. The function of teeth is largely dictated by their shape, and so formal and historical constraints on morphology may prevent a perfect functional form from coming into being. The importance of enhanced tooth function in the evolution of mammals has long been assumed, but how close mammalian teeth are to a perfect functional shape is not known, because criteria for judging perfect shape have never been formulated.

*Corresponding author. E-mail: alistair.evans@sci.monash.edu.au

Maynard Smith *et al*. (1985) suggested the use of '*a priori* adaptive predictions' to detect the presence of constraints on form. Where quantitative predictions of the form expected due to selection can be made, these can be compared to forms in nature. 'A fit with such predictions indicates an absence of relevant developmental constraints strong enough to counteract selection, whereas departure from prediction indicates their presence at least locally' (Maynard Smith *et al*., 1985: 275). Although this was discussed in the context of developmental constraints, it could be extended to apply to any type of constraint, including functional.

The hypothesized shape can be considered an 'ideal' form: a morphology predicted to be the best functional shape according to knowledge of the relationships between shape and function. To construct an 'ideal' morphology, a priori constraints are applied to a form. These will usually include geometric constraints (limitations of three-dimensional space) and functional factors that relate shape to function. For the example of jaw mechanics mentioned above, the 'ideal' form for the position of adductor muscles in terms of mechanical advantage of the muscles would be as far from the fulcrum as possible.

To generate predicted functional forms, it is necessary to understand the relationships between shape and function. The present study concerns the function of teeth as tools for breaking down food (following Osborn & Lumsden, 1978; Lucas, 1979; Lucas, 1982; Lucas & Luke, 1984) and so requires knowledge of how tooth shape affects this function. Shape parameters that can be used to relate tooth shape to function were obtained from tools engineering and functional dental literature. Model teeth were constructed by incorporating the advantageous functional characteristics into basic starting tools to arrive at ideal shapes. The models show how these parameters interact in the form of an 'ideal' morphology that accommodates the functional constraints as well as possible, without the hindrance of developmental constraints.

Two additional geometric criteria imposed by an oral environment that may affect the tools' shape and function (serial repetition of tools and lateral movement) were also introduced to investigate the influence of these factors on tooth shape. Three-dimensional models were created in virtual computer space to fully account for the influence of geometric constraints. If the ideal and real tooth shapes are in close agreement, then we can conclude that other constraints do not substantially impede the fulfilment of the good functional features examined here.

Biological morphology is the result of complex interactions between physical principles and biological evolution at extremely diverse physical scales. Breaking apart and examining these interactions, using techniques such as the construction of 'ideal' morphologies that incorporate the factors constraining them, will give clues to underlying basic rules of form and function in biology, and a much greater insight into the functional aspects of that important mammalian attribute: complex tooth morphology.

MATERIAL AND METHODS

Definitions

This paper will consider the function of a tool in dividing 'tough' foods (that resist crack propagation; Strait & Vincent, 1998). Dietary items that can be considered to have high 'toughness' are found in very diverse taxa: from vertebrate muscle, tendons and skin, invertebrates (including much of the cuticle) to many plant structures (Lucas & Luke, 1984; Strait & Vincent, 1998). The model shapes will be derived without reference to particular food types (e.g. plant or animal material). Specific food types with additional properties may impose other functional demands that would further constrain ideal forms.

The function of a tool is to fracture the food, usually by being driven through it. This can be called 'forced crack propagation', or when performed by a blade, it is often termed 'cutting'. Mammalian teeth, particularly anterior ones, may be adapted for functioning in ways not related to dividing food (e.g. grooming or display), but only function relating to food division will be considered here.

In examining fundamental tooth shapes as topographic features, Lucas (1979) defined a 'point' as a surface with minute dimensions, and a 'blade' as a surface narrow in one dimension. Here, a 'point' will be defined as a location on a convex surface with high (local maximum) curvature in all directions on a two-dimensional surface. A 'blade' is one with high curvature (essentially equal local maxima of curvature) in one dimension, with substantially lower curvature (i.e. close to flat) in the surface at approximately right angles to that direction. The end of a 'blade' may also be considered a 'point' in that there is no direction along the surface where the curvature is essentially zero (as is the case with a blade). 'Cusps' and 'crests', the biological analogues of the idealized shapes, have essentially the same topography as 'point' and 'blade', respectively, in terms of local maxima and minima of curvature. However, there is a diversity of biological shapes, and so to simplify the modelling process below, cusps and crests of real teeth will be modelled as points and blades, respectively.

Factors that are important in the function of points or blades, as discussed in either the biological or engineering literature, are outlined below, along with the reason why they are considered important. Despite many of these functional characteristics having been

individually recognized before, they have not been assembled in a comprehensive analysis that defines ideal functional forms.

Point function

One of the major functions of a tool for dividing tough food is its ability to penetrate and drive through the food. Two major attributes of a pointed tool contribute to this function.

Tip sharpness. The stress required to initiate a crack will vary as the surface area of contact between the tool and the food. Tip sharpness is measured as the radius of curvature at the tip of a point, so a point with higher tip sharpness has a smaller radius of curvature (Evans & Sanson, 1998). A smaller radius of curvature will give a smaller area of contact (for a given elastic modulus of the food), and so produce a higher stress in the food (Lucas, 1982). Freeman & Weins (1997) and Evans & Sanson (1998) demonstrated that increased tip sharpness significantly decreased the force and energy required to penetrate foods.

Cusp sharpness. Once a point has initiated a crack in a tough food, it must be continually driven into the food to sustain propagation of the crack. The force and energy required will in part depend on the volume of the tool and the amount of food displaced. This can be quantified as 'cusp sharpness', which is inversely proportional to the volume of the point at increasing distances from the tip (Evans & Sanson, 1998). A point with higher cusp sharpness has a smaller cusp volume for a given distance from the tip. Increased cusp sharpness reduces the force and energy required for the tooth to drive through a tough food as fewer bonds in the material need to be broken or strained. Evans & Sanson (1998) demonstrated the functional importance of cusp sharpness, where decreased cusp sharpness increased the force and energy to drive a tooth through food.

Blade function

Criteria considered important to the function of a bladed tool are now defined. This list is as exhaustive as possible, and to our knowledge is more extensive than any other in the literature to date. Justifications for each of the criteria are given, based on engineering principles and previous dental modelling.

Edge sharpness. The edge sharpness of a blade is the radius of curvature of the blade edge. A blade with a smaller radius of curvature will have higher edge sharpness, analogous to the 'tip sharpness' of a point. Higher edge sharpness will decrease the area of contact and so increase stress in the food. The importance of edge sharpness was discussed by Frazzetta (1988) and Popowics & Fortelius (1997).

Rake angle. The angle between the leading (rake) surface of a tool and a line from the edge running perpendicular to the direction of tool movement is the rake angle (Fig. 1A). A blade with a positive rake angle (Fig. 1B) has its leading surface angled away from the material to be divided. Compared to a blade with negative rake, less force is required for such a blade to fracture food for a number of reasons. First, a negative rake blade generally must displace more material than one with positive rake, and so requires greater force and energy. Second, the surface area of contact between the food and a blade with negative rake will often be greater, and so a positive rake blade will result in higher stress for a given force. Third, the rake angle affects the force required to keep occluding blades together. When a rake surface contacts food, the blade will tend to be pushed in the direction perpendicular to the surface. Therefore, blades with a negative rake will be pushed apart when food is trapped between them, whereas a positive rake angle directs a blade towards its opposing blade.

Osborn & Lumsden (1978) discussed the functional implications of rake angle. The rake angle of a blade has been shown to have a significant influence on the force and energy to divide food when dividing biological materials (in particular, leaves): a blade with a 30° rake angle required significantly less force than those of 15° or 0° (N. Aranwela, pers. comm.). Rake angle is a common variable in cutting tool engineering, and is a principal measure of the shape of machining tools (Pollack, 1976; Ostwald & Muñoz, 1997; Nee, 1998).

Relief angle. The angle between the direction of tooth movement and the trailing (relief) surface is the relief angle (Fig. 1A). Relief behind blades (also called 'clearance' in some engineering texts) reduces the effect of blades being forced apart by material caught between them, which would require greater force to maintain the proximity of crests. It also reduces friction due to blade–blade and blade–food contact due to food caught between the blades. Once sufficient relief is attained, no further benefit is achieved by increasing the angle, e.g. between 4° and 7° is best for sharp metal or glass sectioning blades shearing plant material for histology sections (Atkins & Vincent, 1984).

Relief angle has been noted by some workers in dental morphology (Osborn & Lumsden, 1978). It is common in the engineering literature, being another basic measure of machining tools (Pollack, 1976; Ostwald & Muñoz, 1997; Nee, 1998).

Approach angle. The approach angle of a blade is the angle between the long axis of the blade and a line perpendicular to the direction of movement (Fig. 1C). The mechanical advantage (MA) of a blade will depend on the approach angle (α) of the blade, where $MA = 1/\cos(\alpha)$ (Abler, 1992; Evans & Sanson, 1998), so that a

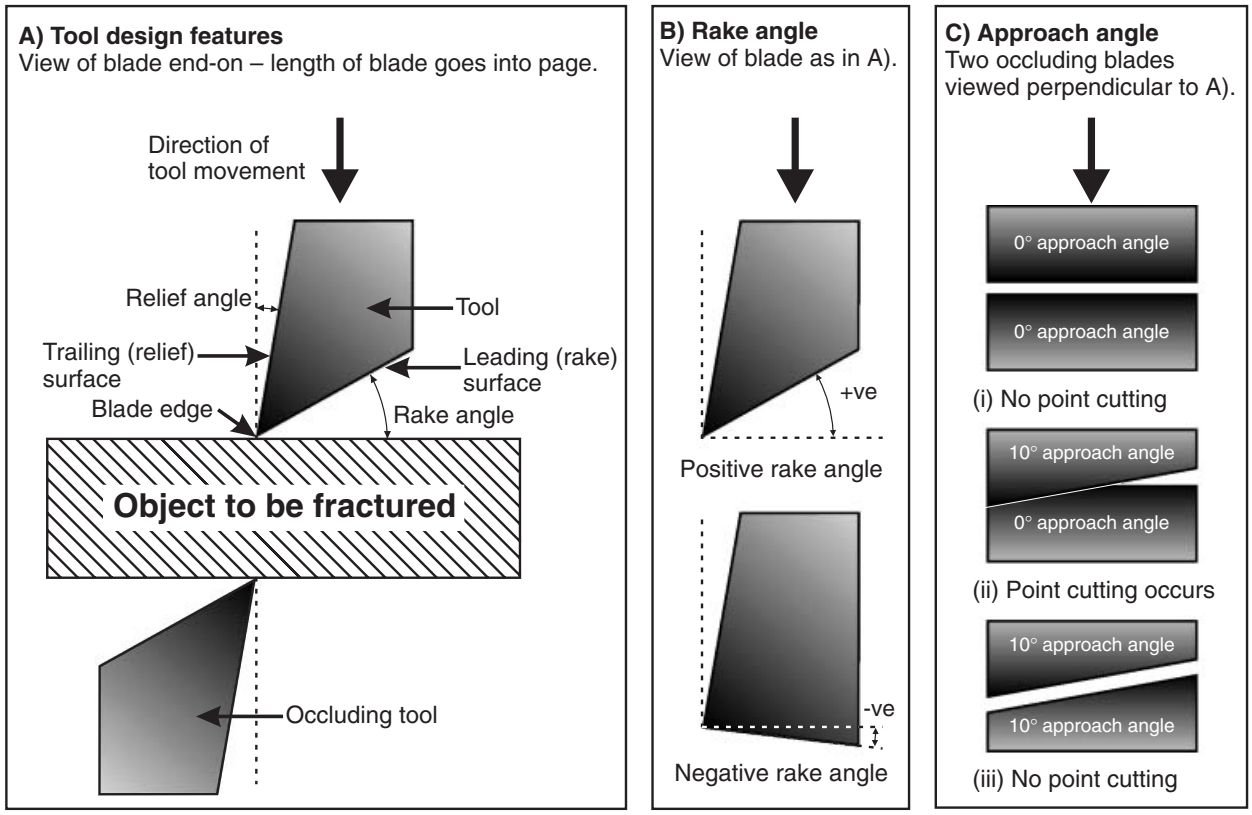

Figure 1. Tool design features. (A) Basic tool design features: leading surface, trailing surface, rake angle, relief angle. (B) Positive and negative rake angles. (C) Variation in the approach angle of two occluding blades and the effect on point cutting.

larger angle will have a greater mechanical advantage. The approach angle of blades will affect the 'point cutting' of the system, which occurs when the long axes of two occluding blades are not parallel, so that only one point (or two points if at least one blade is concave) meets at a time rather than the entire length (Fig. 1ii). Point cutting will decrease the amount of blade trailing surface area in contact at any one time (if there is no relief), which will increase pressure and decrease friction between the blades. Point cutting does not imply that the blade only fractures food at one point at a time, as fracture (or failure or deformation) of food will occur along the entire length of the blade in contact with food, but usually not simultaneously at all points. This is analogous to cutting thick rubber with a pair of scissors: the majority of the material is divided before the blades are close to one another (Abler, 1992).

Approach angle has been discussed by only a few authors in reference to teeth (Abler, 1992; Evans & Sanson, 1998), and point cutting by many others (e.g. Crompton & Sita-Lumsden, 1970; Seligsohn, 1977). The effect of approach angle on the required occlusal force has been measured for sharp blades (Abler, 1992) and facsimile tooth crests (Worley & Sanson, 2000). In machining tools, it is called the inclination angle (Cubberly, 1989; Nee, 1998).

Food capture. Food is more likely to be completely divided if it is trapped between blade edges, preventing it from escaping off the ends of the blades and therefore being incompletely divided. Blades can be concave so that the ends meet first, enclosing the food before it is then fully divided. This is particularly relevant in foods with a very high Poisson's ratio (ratio of the strains perpendicular and parallel to the force; Lucas & Luke, 1984), which may be hard to trap between blades. A crest may be notched or curved (a sharp or rounded concavity, respectively). The functional advantages of capturing food have been recognized for many tooth forms (such as carnassial and tribosphenic; Van Valen, 1966; Savage, 1977; Freeman, 1979; Abler, 1992).

Fragment clearance. The function of blades will improve if the fractured material is directed away from the blades and off the rake surfaces. If material

is trapped on rake surfaces, this may prevent fracture of food caught between blades. Where there is insufficient space into which fractured material can flow, food may be compressed between opposing tooth structures and prevent the occlusion of crests. This becomes more relevant where blades on the same tool are closer together, resulting in a greater chance of food being caught between two opposing surfaces. In such circumstances, it is advantageous to create flow channels and exit structures to direct flow of food away from the blades and off the occlusal surface.

The movement and clearance of food has been given some attention in the dental literature: food movement was incorporated into Rensberger's (1973) models of herbivore teeth; Seligsohn (1977) discussed it in terms of food escapement; Sanson (1980) as sluiceways; and Frazzetta (1988) noted the clearance provided by 'gullets' between successive multiblade or serrated edges of teeth. In single point machining tools, an analogous process of chip clearance may be carried out by a change in inclination angle or by a chip breaker (a groove ground into the rake face of the tool that breaks chips into smaller pieces, allowing them to be thrown clear; Nee, 1998; Pollack, 1976).

Modelling tool shapes

Models of forced crack propagation tools can now be devised using the criteria outlined above. The objective is to examine the key principles related to shape and function of these tools, and the limits they place on possible tool shapes.

Functional parameters

Single-bladed tool. The first system to be modelled is a tool with a single blade. The basic shape for such a tool need only be a block that meets an opposing tool along one edge (the blade) of each block (Fig. 2A). Each blade is linear, with 0° rake, 0° relief, 0° approach angle and no capture, so the entire length of one blade meets the opposing blade at the same time. As a simplification, the tools move relative to each other in a vertical linear motion, so the blades move past one another rather like a guillotine. Each tool will occlude with another tool of the same shape to limit the number of possible tool combinations. It is assumed that fracture of the tools themselves is not possible, i.e. the tools have infinite strength. The influence of tool strength on shape is discussed later.

Our interest lies in variations of this basic tool shape. The inventory of all single-bladed tools with every conceivable variation in blade shape (the 'morphospace' for bladed tools) is too large for all shapes to be examined. Instead, we will define 'shape parameters', which are the 'dimensions' in which the shape of the tool can vary. For instance, one shape parameter is the radius of curvature at the tip of a point, and so a point tip can have a large or a small radius of curvature. The functional parameters relate the shape parameters to the function of the tool, so that the 'tip sharpness' of a point is the radius of curvature at the tip. The optimal state for each shape parameter (called the functional criterion) can be deduced from the functional parameters; in this instance, a small radius of curvature is advantageous for penetrating foods. The list of shape parameters, along with the corresponding functional parameters and criteria, is given in Table 1.

Most of the shape parameters can vary continuously, from either small to large, or positive to negative. Instead of examining the continuum, only two or three states for each of these are examined here, usually at the extremes of the continuum, e.g. for rake angle, negative, zero and positive angle; for relief

Table 1. Shape and functional parameters for points and blades. For each shape parameter, the possible states (e.g. small/medium/large) are listed, along with functional parameter that relates the shape to its function. The optimal state of each shape, according to the functional parameters, is also shown

Shape parameter	Possible states for shape parameters	Related functional parameter	Optimal shape state (functional criterion)
Radius of curvature of point tip	Small/medium/large radius	Tip sharpness	Small radius
Volume of point	Small/medium/large volume	Cusp sharpness	Small volume
Radius of curvature of blade edge	Small/medium/large radius	Edge sharpness	Small radius
Angle of leading surface of blade	Negative/zero/positive angle	Rake angle	Positive angle
Angle of trailing surface of blade	Zero/positive angle	Relief angle	Positive angle
Arrangement of blade edge	Zero/positive angle	Approach angle	Positive angle/point cutting present
	Relative heights of A, B and C: No capture/capture	Food capture	Capture present
General arrangement of rake surfaces	Trap food on rake surface/ clear food off rake surface	Fragment clearance	Clear food off rake surfaces

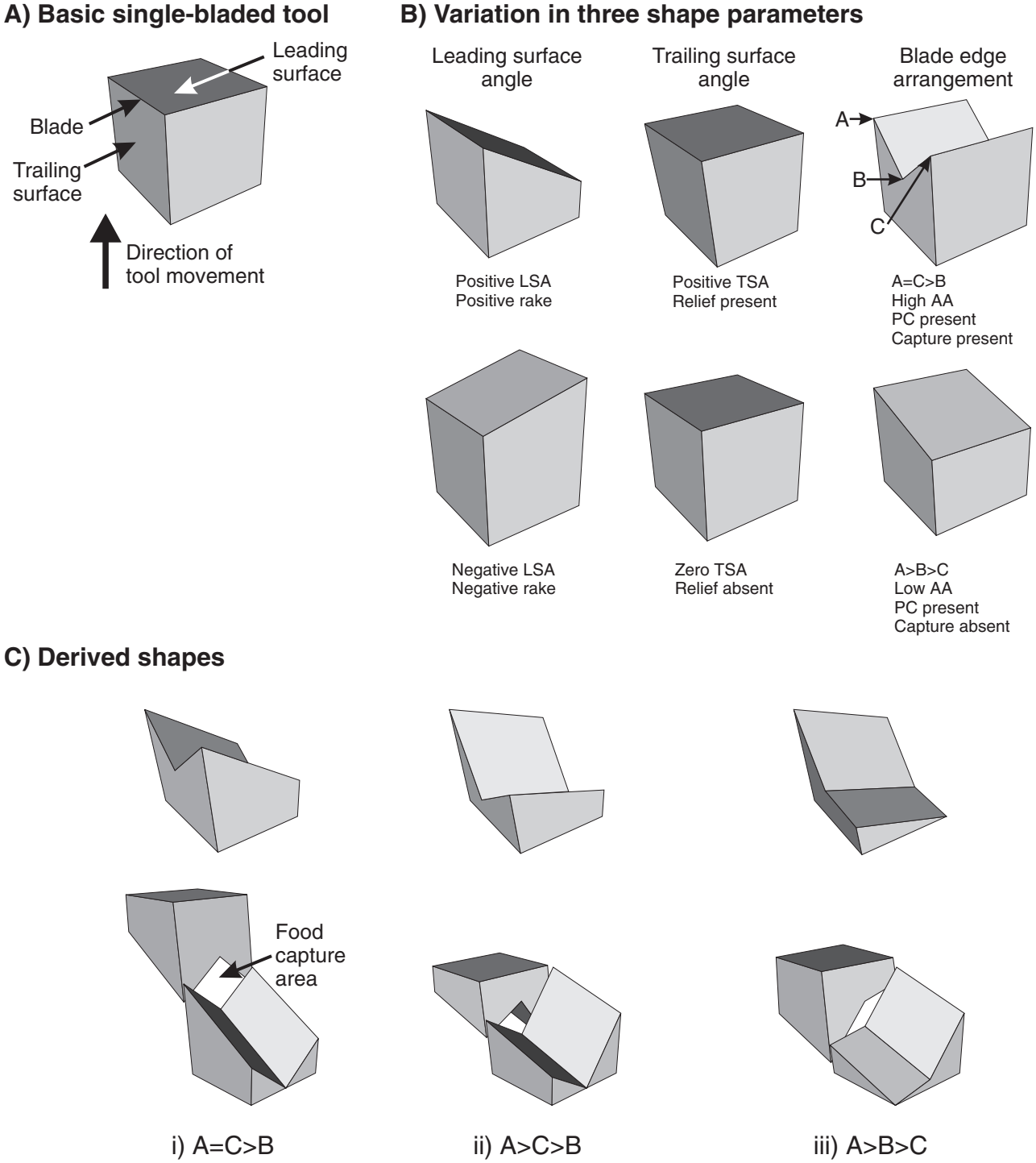

Figure 2. Single-bladed tool shapes and shape and functional parameters. (A) The basic single-bladed tool has a single blade with 0° rake, 0° relief, 0° approach angle, and moves vertically. The blade on the tool is indicated. (B) Three of the shape parameters are altered: the angle of the leading and trailing surfaces and blade edge arrangement. (C) The derived shapes fulfil all eight functional criteria: tip, cusp and edge sharpnesses, rake, relief, capture, approach angle and fragment clearance. Each tool is shown singly and as it would occlude with another tool of the same shape. Abbreviations: A, B, C are apices A, B and C, respectively; LSA, leading surface angle; TSA, trailing surface angle; AA, approach angle; PC, point cutting.

angle, zero and positive angle. Blade edge arrangement cannot be considered in this way. Instead, the edge of the blade is defined by the positions of both ends (Apices A and C) and a middle point (Apex B) along the blade (Fig. 2B). The three apices lie in a vertical plane, ensuring that the edges of occluding blades meet.

Three-dimensional reconstructions of the tool models were created using Virtual Reality Modelling Language (VRML), a relatively simple programming language for three-dimensional computer modelling (e.g. Evans, Harper & Sanson, 2001). Model shapes were constructed using the 'IndexedFaceSet' command, where the three-dimensional coordinates of the tools are specified. A VRML browser such as 'CosmoPlayer 2.1' (Computer Associates International, Inc., Islandia, U.S.A) can be used to view the models and manipulate them in virtual three-dimensional space to illustrate that proper occlusion occurs. All figures of the models (Figs 2–4) are from the VRML reconstructions. The purpose of VRML is to illustrate the 3-D morphology of the shapes and to test geometric hypotheses (i.e. that occlusion between blades occurs as predicted). It is not designed to specifically test the function of the tools in terms of force required to function, as this is assessed according to the functional parameters.

Starting with the basic tool described above, tools were created with all combinations of relative heights of Apices A, B and C (e.g. A = B = C, B > C = A, C > A > B). Each of these was assessed for point cutting and capture ability (the functional parameters related to blade edge arrangement). For the shapes that fulfil these two criteria, the remaining shape parameters were altered to correspond to the functional criteria. For instance, both rake and relief angles of the blades are modified from 0° (the state of the basic tool) to a positive angle. Some features do not need improvement from our basic shape (such as edge sharpness, as the edge has an infinitesimal radius) or may improve in parallel with change in others (such as approach angle, which can vary with capture). Figure 2B shows the effect on the shape of the tool when some of the shape parameters are altered individually.

Double-bladed tool. The model of a double-bladed tool used here has two blades set at an angle to each other, like a prism with an equilateral triangle at the base and top (Fig. 3A). Two of the edges on the top surface act as blades that occlude with blades of other tools. This design fits two blades in the space (or more precisely same tool length) of the previous one, with a greater combined blade length. Shapes other than the prism could be used (such as the cubic single-bladed tool, where two adjacent edges are blades), but the particular choice of starting tool does not affect the final conclusions.

The morphospace for double-bladed tools is even larger than that of single-bladed tools. The junction of the two blades is Apex A, the other end is Apex C, and Apex B is in between. The tools made here will be symmetrical around Apex A. As for the single-bladed tool, all combinations of relative heights of A, B and C were constructed. The shape parameters of this tool are now altered according to the functional parameters. Figure 3B shows how several of the shape parameters can be individually modified on the double-bladed tool.

'Anatomical' constraints

In addition to the functional parameters used above, further criteria can be introduced that will influence the way that the tools can be used in real biological systems, that is, they are factors that may influence their shape and function in the mouths of animals. The objective is to see whether the shapes can accommodate these additional criteria, and to what degree they must be modified to do so.

First, we will create multiple functional copies of the tools, approximating many teeth in a jaw. The easiest way to do this is to arrange several of them serially, as if in a tooth row.

Second, we will introduce a degree of lateral movement, which is advantageous for several reasons. If a tooth in the mouth of an animal moves directly vertically, there may be a tendency for food to become trapped between the teeth or non-tooth structures (e.g. the jaw or palate), preventing the blades from coming into contact. Also, food may be forced into the gums of the opposing tooth row. The possibility of this occurring would be reduced by some amount of lateral movement of the opposing teeth, so that the vector of movement of the teeth (the occlusal vector) is now vertical with a lateral component. This is essentially extending the fragment clearance criterion to include prevention of food trapping between tooth and non-tooth structures.

RESULTS

Functional parameters

Once the shape parameters of the tools have been altered according to the procedure above, the result is the subset of tool morphospace that fulfils the functional parameters. For each type of tool, several different designs may meet all of the functional criteria, as there may be multiple blade edge arrangements that allow for capture and point cutting.

Single-bladed tool

The single-bladed tool shapes shown in Figure 2C fulfil the eight functional criteria. The three different tool

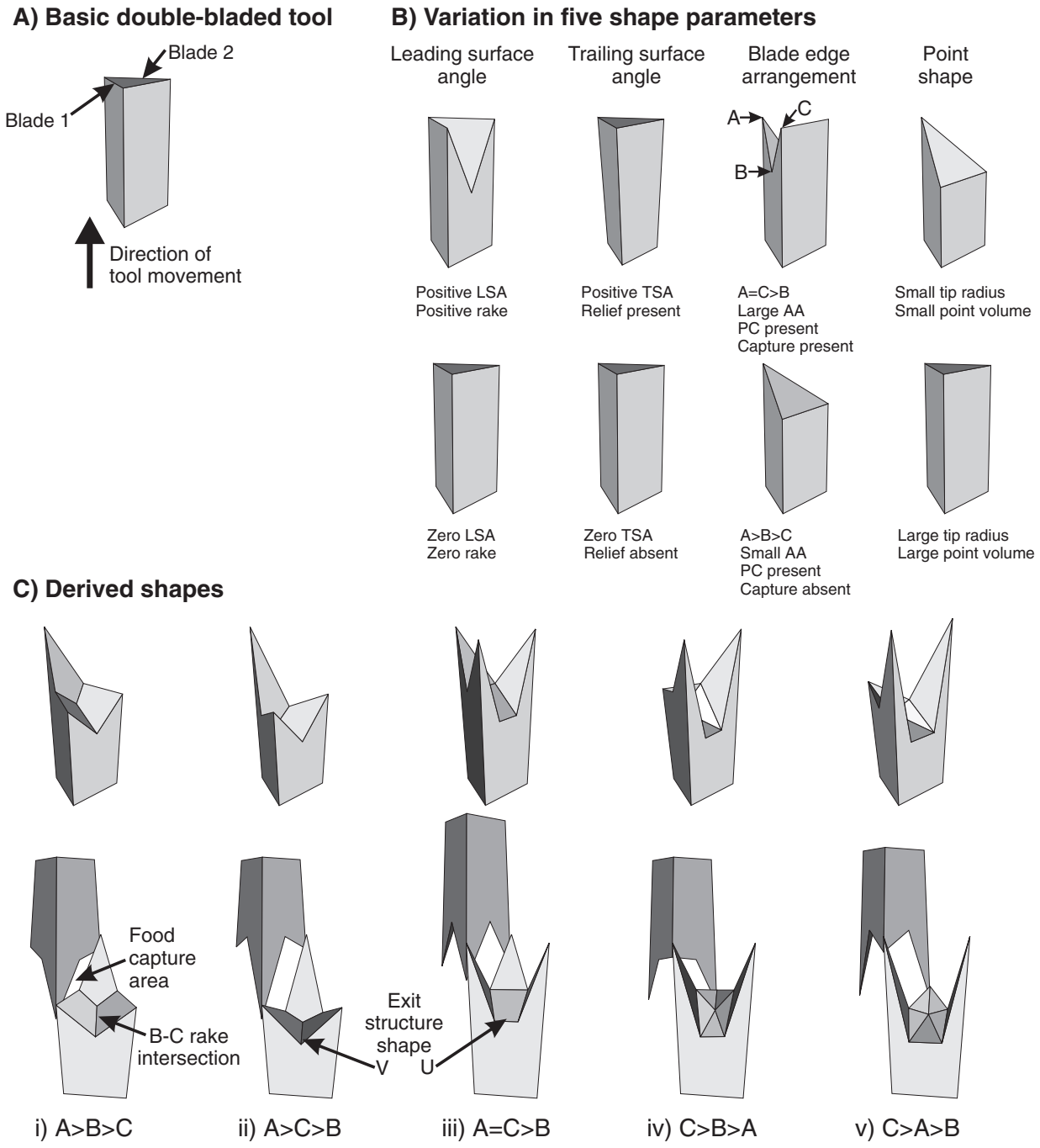

Figure 3. Double-bladed tool shapes and shape and functional parameters. (A) The basic double-bladed tool has two blades, each with 0° rake, 0° relief, 0° approach angle, and moves vertically. The two blades on the tool are indicated. (B) Five of the shape parameters are altered: the angles of the leading and trailing surfaces, blade edge arrangement and point shape (which includes both tip radius and cusp volume). (C) The derived shapes fulfil all eight functional criteria: tip, cusp and edge sharpnesses, rake, relief, capture, approach angle and fragment clearance. Each tool is shown singly and as it would occlude with another tool of the same shape. See Fig. 2 for abbreviations.

types in Figure 2 are: (i) the ends of blades are equal in height (A = C > B) and the tool is symmetrical; (ii) one end is the tallest apex, followed by the other end, with the notch the lowest (A > C > B); and (iii) the ends represent the maximum and minimum of the blade height, with the notch in between, but B is lower than the line A–C (A > B > C). These blades allow for capture (as they are 'notched' so that they enclose some area for food capture) and point cutting. All other possible shapes do not allow for capture when occluded with a tool of the same shape (e.g. B > A > C) or have zero approach angles for some length of the blade (e.g. A > B = C).

Double-bladed tool

The general shapes that fit the functional criteria are shown in Figure 3C. The first three tools are: (i) primarily single-pointed, with the notch in each blade higher than the lateral points (A > B > C); (ii) one maximum point and two lower points, with the notch lower than lateral points (A > C > B); and (iii) a three-pointed design (A = C > B). These are essentially the double-bladed versions of our single-bladed tools, where the notch apex may be lower (C > B) or higher (B > C) than the lower end of the blade, but always lower than the line A–C. In these three tools, the highest points of each of the blades meet at the same point on the tool (A).

The other two derived shapes in Figure 3C (iv,v) differ topographically from the first three in that the junction of the blades (Apex A) is not the highest point of the tool. Good rake angles for these shapes can only be achieved by directing the rake surface deep into the body of the tool.

Once material has been divided, it must move off the rake surface to allow further fracture to occur (the 'fragment clearance' criterion). When two blades are placed on the same tool, this may be more difficult as the directions in which the material can flow are further limited. For the double-bladed tools, the third edge of the top triangle has become an 'exit structure' (Fig. 3C) out of which divided material must flow. In designing these tools, the junction between the rake surfaces of the B–C segments of the blades (B–C rake intersection; Fig. 3C) could have been made horizontal. However, to improve the flow off the rake surfaces, it has been sloped away from the blades into the exit structure.

The shape of the exit structure differs between these tools. A U-shaped exit structure was used for 3iii as a greater volume of material will probably be divided by this shape as shown by the greater capture area. For 3iv–v, the proximity of the rake surfaces of the two blades near Apex A may restrict flow, so a larger U-shaped exit area was provided.

'ANATOMICAL' CONSTRAINTS

Serial arrangement

Single-bladed. This can easily be achieved for our single-bladed tools. The simplest arrangement is to place the tools in a line so that the blades are parallel to the row of tools (the tooth row). This creates a continuous cutting edge that is zig-zag in the vertical direction, giving the appearance of a serrated blade.

Double-bladed. The double-bladed tools can be arranged serially so that the blades form a continuous, jagged cutting edge, and each tool occludes with two others.

Overall, both of these tool types can be arranged serially without the need to modify their shapes.

Lateral movement

Single-bladed. A moderate amount of lateral movement is easily accommodated into these designs. A great amount is probably not necessary to avoid compression of food with this tool design, as there is less of a problem with food being trapped on the rake surfaces. The main feature that must be altered is the orientation of the blades. For blades that move along a linear trajectory, the easiest arrangement is for the entire length of the blade (the three apices, including the notch defined by B) to be in a plane that includes the vector of tooth movement (i.e. occlusal vector is perpendicular to the normal of the plane). The vertically moving tools fit this pattern, as the occlusal vector is vertical and each blade lies in a vertical plane. Therefore, when blades are arranged to introduce some lateral movement, they must be in a plane that includes the occlusal vector. Also, for blades on two different tools to occlude, they must be orientated in the same plane (which is not guaranteed, as there are infinitely many planes with normals that are perpendicular to a given vector). When the blades are concavely shaped, food will be captured between the blades and there will be at most two point contacts between the occluding blades (Fig. 4i).

Double-bladed. The double-bladed tools can only move laterally in one direction, so that the original rake surface is still the leading surface of the tool. This means that Apex A of one tool moves vertically and laterally in the direction of Apex A of the opposing tool. If the tool moves in the other lateral direction (so that the relief face becomes the leading face, and A moves towards C of the opposing tool) then the tool will run into the junction between the two tools it occludes with.

Introducing lateral movement into the double-bladed system is slightly more complicated than the

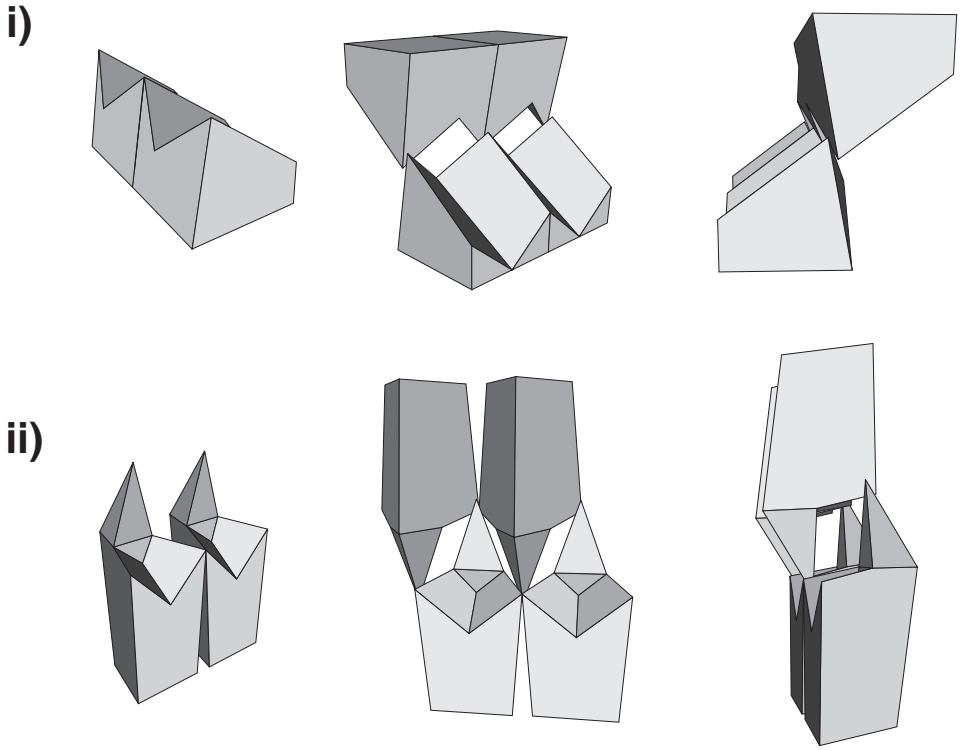

Figure 4. Anatomical criteria for tool design. Single-bladed (i) and double-bladed (ii) tools arranged serially and with lateral movement.

single-bladed, but the same principles apply. For two blades to occlude, they must be in the same plane that includes the occlusal vector. If there are multiple blades on a tool (e.g. two), the intersection between the two blade planes will be a line, and this line will be parallel to the occlusal vector.

For the one-pointed double-bladed shapes (3i,ii), shifting the tip of the main point (A) towards Apex C ensures that it is pointing closer to the direction of tooth movement. This will improve penetration by the main point, aid in the rearrangement of the blade planes so they include the occlusal vector, and improve the rake angle of the blades leading down from the main point (Fig. 4ii).

Lateral movement with a three-pointed tool (3iii) and the other two-bladed shapes (3iv,v) is more difficult. It is possible to reconfigure them so that the blades will contact throughout the stroke, but the degree of lateral movement will be more restricted when compared to the one-pointed shape.

VRML files for some of the single-bladed (4i) and double-bladed (4ii) tools are given in the Appendices. These include the three-dimensional coordinates of the shapes and the vectors of tooth movement, and allow the full three-dimensional shape and occlusion of the tools to be viewed.

DISCUSSION

Considering all of the tools in the large eight-dimensional tool morphospace examined here, there are only a few tool designs that are able to fulfil the constraints imposed by geometry and those dictated by the functional parameters. The shapes derived above will now be examined in more detail.

Functional merits of model tools

The shape parameters of the tools have been altered to conform to the functional criteria for point and blade function. This makes them highly effective tools for the fracture of food by forced crack propagation, as the force and energy required for them to divide food should be minimized or at least reduced compared to the starting tools. Once anatomical constraints are also incorporated into the designs (Fig. 4), the models are capable of being accommodated in the mouth of an animal, at least for the simple instances considered.

Despite the fact that all of these tools do fulfil our functional criteria, they are not functionally equivalent for several reasons. Some of the tools (2ii,iii, 3i,ii) have a single maximum point that will be the first to contact the food and initiate a crack; others have two

(2i, 3iv,v) or three (3iii). A one-pointed design may be more advantageous in terms of force (having only one initial point as opposed to three, and so produce three times the stress for a given force). However, crack initiation and propagation at a greater number of points may allow faster fracture of food.

The tools also differ in the extent to which they can fulfil the functional requirements. For the single-bladed tools, large approach angles and capture areas are easier to achieve for design 2i than for 2ii and 2iii. For the double-bladed tools, it is difficult to achieve a good rake angle for tools 3iv,v (especially at Apex A, where the rake surface must be directed deep into the body of the tool) compared to tools 3i–iii. Lateral movement is more restricted in shapes 3iii–v and further compromises the rake angles of 3iv,v. From this, it appears that the first two shapes (3i,ii) are the best designs for our criteria and most closely approach our 'ideal' functional tooth shape.

We will coin a new term for the final double-bladed tool with one maximum point: *protoconoid*, taken from '*proto*' meaning 'first or primitive', '*con*' from 'conus' meaning 'cone' and '*oid*' meaning 'like'. This is not to be confused with *protoconid*, the main cusp on lower tribosphenic teeth. The protoconoid is not a single cusp or point, as the name may imply—it is a functional complex consisting of a specific arrangement of points, blades and the surrounding tooth surface. The term 'protoconoid' will be used to refer to both the vertically and laterally moving tools (3i,ii, 4ii), as they all possess common functional benefits, as listed in Table 2.

Relationships between model shapes and real tooth shapes

After specifically disregarding the shapes of real teeth in designing our model tools, it is now interesting to consider how similar the derived functional shapes are to shapes that occur in animal teeth. Comparison between the teeth of animals and the models created here, based solely on a priori assessments of the factors that will affect the function of forced crack propagation tools, reveal many similarities and consistencies. Correspondence between shapes can be assessed in terms of topography of the teeth (the position and arrangement of cusps and crests) and how well they fit the functional criteria, which will be reflected in the fine details of tooth surface shape.

Table 2. The important functional advantages of the protoconoid

1	Initial penetration by a single maximum point with high tip and cusp sharpness
2	Forced crack propagation along blades
3	High edge sharpness of blades
4	Blades with positive rake angle
5	Relief present behind blades
6	Ability to capture food between blades for fracture
7	Good approach angle and point cutting
8	The presence of an 'exit structure' to allow food fragments to flow off the rake surfaces of the blades
9	Many copies can be placed serially to form a tooth row
10	A degree of lateral movement is easily accommodated

General topography

There are many tooth shapes that are topographically equivalent to the single-bladed tools. The symmetrical single-bladed tool (2i; Fig. 5A) is comparable to a carnassial (Savage, 1977; Mellett, 1981; Van Valkenburgh, 1996), both having a single blade with a large notch and cusps at each end (Fig. 5C). The carnassial tooth form is a relatively common tooth shape found in several diverse carnivorous lineages, particularly carnivorans (formed by the fourth upper premolar and first lower molar: P^4/M_1) and the extinct creodonts ($M^{1–2}/M_{3–4}$).

The asymmetrical tools (2ii,iii; Fig. 5A) appear in many more settings, such as the premolars of animals with tribosphenic-like teeth and in carnivores (Fig. 5D; Freeman, 1981; Mills, 1966). The general form of these premolars is a single asymmetrical blade. The crests of all of these teeth have the middle apex of the crest (B) lower than a straight line connecting the ends (A and C), allowing capture of food between the blades.

The topography of the protoconoid designs (3i,ii, 4ii; Fig. 5B) greatly resembles many cusp-crest complexes of real tooth forms, such as zalambdodont (found in some insectivorans, e.g. tenrecs), dilambdodont (many microchiropterans and insectivorans, e.g. shrews and desmans) and tribosphenic molars (some primitive mammals and many insectivores, e.g. opossums) and several extinct groups (e.g. symmetrodonts and pantotheres) (Fig. 5E; Mills, 1966; Crompton, 1971; Freeman, 1981). The main cusp structures of these teeth (for upper tribosphenic molars, paracone and metacone, and lower molars, protoconid and to a lesser extent hypoconid) have a basic protoconoid shape. For all of these complexes, there is a single, tallest cusp that is the junction of two crests. Each crest is asymmetrical, with the ends of crests at unequal heights, and concave, allowing capture. Cusps are present at the lower end of each crest (e.g. parastyle, paraconid in tribosphenic molars).

Functional parameters

The carnassial and tribosphenic tooth forms also have great similarities in the detailed shape of the tooth surface with the single- and double-bladed models. For instance, the crests of most carnassial and tri-

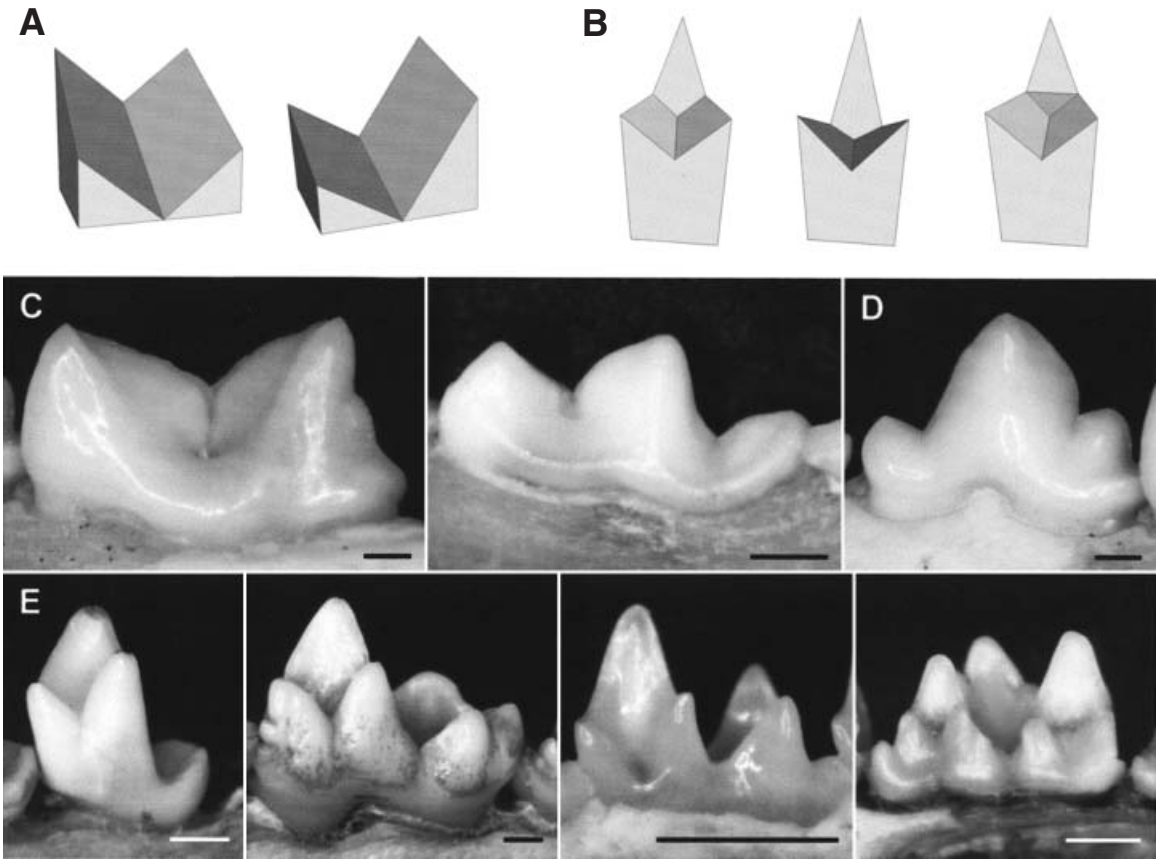

Figure 5. Comparisons between the models and real mammalian tooth forms. L–R. Model tools: (A) single-bladed tools, symmetrical (2i) and asymmetrical (2ii); (B) double-bladed tools (3i, 3ii, 4ii). Mammalian tooth forms: (C) lower carnassials of *Felis catus* (Carnivora: Felidae) and *Mustela frenata* (Carnivora: Mustelidae); (D) premolar of *F. catus*; (E) lower molars of *Tenrec ecaudatus* (Insectivora: Tenrecidae), *Didelphis virginiana* (Didelphimorphia: Didelphidae) and *Chalinolobus gouldii* (Chiroptera: Vespertilionidae), and upper molar of *Desmana moschata* (Insectivora: Talpidae). Scale bars = 1 mm.

bosphenic teeth have a positive rake angle and relief behind the crests (Evans, 2000; Osborn & Lumsden, 1978; Evans, in press; unpublished data). They allow for capture of food and point-cutting (Crompton & Sita-Lumsden, 1970; Seligsohn, 1977; Osborn & Lumsden, 1978; Lucas & Luke, 1984; Evans, 2000; Evans, in press; unpublished data) and have high edge sharpness (Evans, 2000; Freeman, 1992; Popowics & Fortelius, 1997; Evans, in press; unpublished data). Flow of food off rake surfaces is assisted, as the exit structure in tribosphenic cusps slopes away from the blades (Evans, in press; Seligsohn, 1977). In other words, these teeth largely conform to the functional criteria set out above.

'Ideal' forms and constraints

The similarity between real tooth shapes and the ideal functional forms can now be addressed. According to the functional and limited anatomical criteria from which they were constructed, the models are the best possible functional shapes. Their close similarity to animal tooth forms suggests that these teeth have the best shape for their function. Their shape, then, is not substantially limited by developmental constraints – the developmental processes of mammalian teeth allow the construction of essentially perfect functional shapes. Dental morphology has managed to escape whatever developmental constraints apply to it to achieve essentially optimal functional tooth designs, and these teeth are largely shaped by the geometric and functional demands placed upon them. It is interesting to note how often the tribosphenic tooth form is often considered 'unspecialised', apparently in the sense of 'unadapted' to a specific use. In truth, it can be seen how superbly adapted this tooth form is.

Dental evolution has surmounted additional functional demands not considered in this model that may be in conflict with a tooth's food-fracturing function, such as the biomechanical properties of the teeth themselves (Popowics, Rensberger & Herring, 2001).

For example, without being sufficiently strong and stiff, teeth would not be able to fracture most foods without themselves being broken or deformed (Lucas, 1979). The relative strength of the tool and food will influence tool shape. If a weaker material were used to construct the tools, it is likely that the following tool features would be altered: greater robustness of tooth features overall; decreased tip sharpness (rounding of cusp tips); decreased cusp sharpness (shorter, fatter cusps); decreased edge sharpness (rounding of blade edges); and decreased sharp angles in tooth features (e.g. notch in blades would not be as sharp, as the notch would act to concentrate forces and promote tooth fracture). The bulk of the minor differences between the models and teeth can be seen as being due to the influence of tooth strength, but these do not influence the qualitative shape of the tools and the conclusion that they fulfil the functional criteria set out above.

If a rigorous investigation of the effects of tool strength on shape were to be undertaken, a more complicated modelling process would be required that takes into account the stresses generated in both the food and tool when the tool is functioning and relate it to the stresses that each could withstand. This modelling would require more detailed specification of the forms of the tool and food, producing results of reduced generality. Instead, the models constructed here give qualitative shapes in terms of broad topography and functional parameters, allowing large-scale trends to be discerned. Without additional complication, strength can be taken into account in a limited way, such as providing another reason to prefer shapes 3i,ii over 3iii–v, as the latter of these shapes tend to have taller, thinner cusps that risk fracture.

The lack of constraints on morphology can also be detected by convergences in form, which will be independent of the a priori predictions used to create the model (Maynard Smith *et al*., 1985). Tooth forms containing protoconoid-like shapes have persisted in mammals for over 140 million years, being present in early therians (Sigogneau-Russell, Hooker & Ensom, 2001) and extant insectivorans and microchiropterans. Likewise, the maintenance of morphology over a significant time span and wide range of scales could also indicate freedom from constraint. Carnassial forms have been independently derived in several carnivorous lineages (more than five times in fossil and modern carnivorans and twice in marsupials; Butler, 1946). Similar tooth forms are present in animals of widely varying body size, often over three orders of magnitude in body mass, e.g. dilambdodont or tribosphenic (2 g shrew to 2 kg opossum) and carnassial (50 g mustelids to 200 kg lion; body masses from Silva & Downing, 1995).

This final point indicates the likelihood of a very significant feature of these designs that enables them to function at such different sizes: the function must rely on some shape characteristics that are relatively scale-independent. Many of the functional features discussed here are size-independent (e.g. topographic features such as presence of cusps to aid penetration of food and crests for crack propagation; surface shape such as rake, relief and approach angles of crests). Conservation of these features would be expected over large (if not all) size ranges, resulting in the ideal solution being largely identical for all tooth sizes. This is very likely to be the case for the single- and double-bladed tool shapes derived here.

The maintenance of and convergence onto a few tooth forms, and their presence at differing scales, point to the conclusion that development has very little, if any, constraining influence with respect to these functional shapes. It appears that their developmental regime has allowed these functional shapes to be achieved very early in their evolutionary history.

Dietary properties

The physical properties of a food should determine the 'ideal' tooth shape to divide it (Lucas, 1979). The diversity of mammalian diets includes strong bones, tough and viscoelastic meat, high- and low-fibre leaves, and fruits that are hard and strong or weak and juicy. The method of best dividing a food will differ with the type of food, as each food will impose its own functional demands. We would therefore expect a variety of ideal shapes to be found in mammals.

The protoconoid and carnassial shapes appear to be the best functional shapes for a food simply considered as 'tough'. Animals that possess these tooth forms are largely insectivorous or carnivorous (e.g. insectivorans, microchiropterans, canids and felids), which may indicate that invertebrates and vertebrate flesh can be treated as being largely similar in terms of the functional demands placed on tooth form.

A large number of mammalian molar forms is not derivable from the above modelling (e.g. molars of humans and herbivores such as rats, horses and kangaroos). It is likely that this can largely be attributed to the influence of additional constraints imposed by physical properties (e.g. high hardness or strength, brittleness or juiciness) that more greatly influence functional form than toughness for a given food type. The extent to which the food needs to be divided will also influence tooth form.

Although these other forms do not resemble the ideal shapes of this study, this does not indicate that these other forms are not in some sense functionally 'ideal'. The general shapes of ideal tooth forms for other dietary types have been speculated upon

(Osborn & Lumsden, 1978; Lucas, 1979; Lucas & Luke, 1984), but further detailed analysis is required to assess whether there are any major developmental constraints preventing the construction of this ideal form. However, the high degree of parallelism, convergence and size-independence exhibited by these forms suggests they may be 'ideal' for some diet, or as close as can be achieved given non-functional constraints.

Interactions of constraints

As well as the constraints on the shapes of teeth and tools discussed above (geometric considerations, functional and anatomical criteria), interactions between these factors also constrain tooth shape. Altering any criterion may interfere with the optimization of others, or some may be modified in parallel (e.g. approach angle and capture), so that each criterion can only be maximized to a certain extent, generally limited by geometry. Figure 6 is a putative map of the main interactions between the functional criteria and a few other dimensions, showing which criteria are generally affected when others are altered. Three-dimensional blade length is simply the length of the blade in three dimensions (Fig. 6 inset). Functional blade length is the length of a cut made by a blade: the two-dimensional length of the blade projected onto a plane normal to the occlusal vector (PNOV).

An important case where geometry plays a role is where the packing of blades on a tool is increased, usually by the addition of other blades. There are compromises between the advantages of increased packing (a greater amount of food can be divided with one stroke; the breakage function of Lucas & Luke, 1983) and the ability to conform to the functional criteria. Compared to the single-bladed model, increased packing of blades in the double-bladed model means it is harder to fulfil the criteria. Trade-offs will occur, as the function of each blade is more likely to interfere with the function of a nearby blade. For certain blade configu-

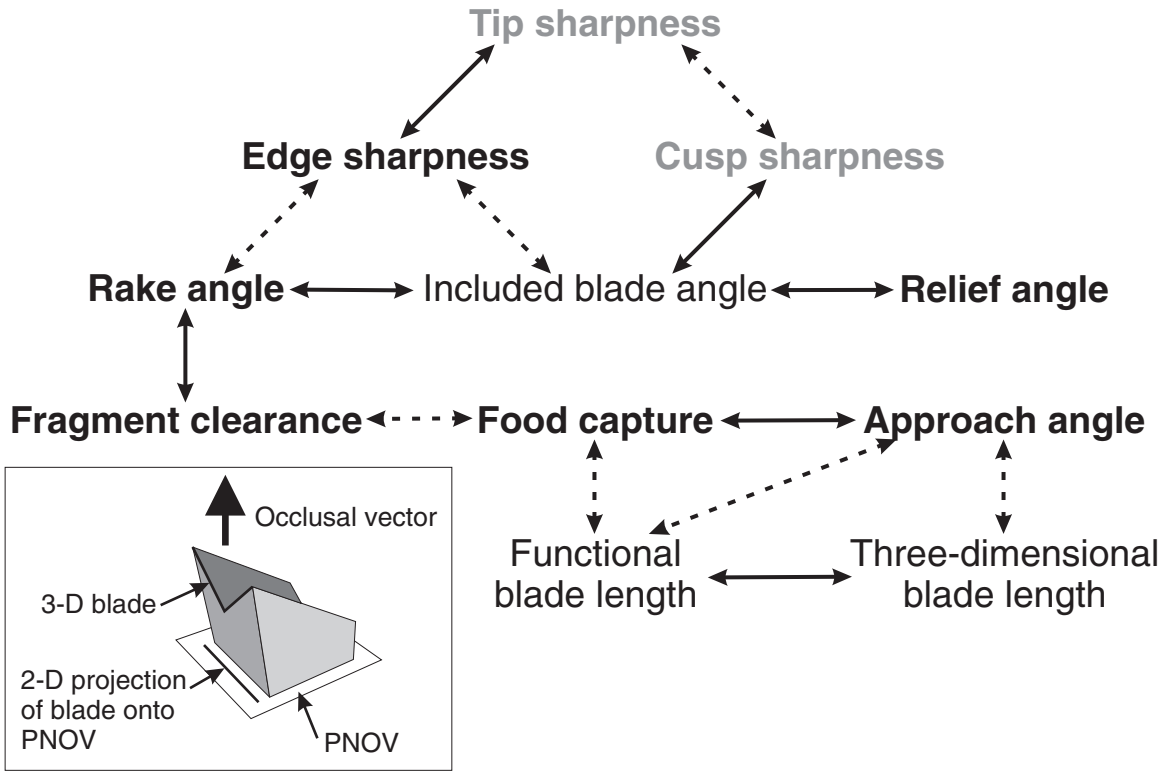

Figure 6. Putative relationships between tooth functional characteristics. Bold characters are the eight criteria considered in this paper, with grey characters affecting points and black characters affecting blades; non-bold characters are other factors that may be considered combinations or derivations of the eight criteria. Solid arrows signify a strong relationship: if one of these features is altered, it has a direct affect on the others; dashed arrows signify a weaker relationship, such as an indirect effect. This shows which other features would change in order to accommodate an alteration in that character. 'Included blade angle' equals (90° – rake angle – relief angle). The other characters are defined in the text.

rations, these interactions and constraints may be more apparent, so that the final tool shape is a compromise of many features. This is demonstrated by tools 3iv–v, where the configuration of the blade edges means that a good rake angle is difficult to achieve.

Tooth modelling

The purpose of this study was to reduce the complexities of mammalian teeth to distil the essential characteristics of a functioning tooth. These include the geometric arrangement of particular components and their ability to function in a given manner. The power of the present analysis lies in the model being fully explicit, where every feature is specifically determined by the functional parameters. Also, each factor that is incorporated is independently justifiable and can be considered and rejected separately, allowing the dissection of the relative importance of each feature. For instance, the effect of approach angle can be individually inspected to show its importance in tooth function, and removed from the model if deemed inappropriate.

This analysis is more detailed than earlier work that has considered the probable form of tooth structures for given dietary properties (Osborn & Lumsden, 1978; Lucas, 1979; Lucas, 1982; Lucas & Luke, 1984) in its consideration of shape factors that affect the function of teeth. This is presumably the reason for the greater degree to which the current model tools approach the shapes of mammalian teeth. The shapes derived here can be further examined through other types of analysis, such as computer modelling of forces (e.g. finite element analysis; Rensberger, 1995; Spears & Crompton, 1996; Spears & Macho, 1998) or empirical force-testing of alternative tool shapes (Abler, 1992; Evans & Sanson, 1998), to substantiate the results obtained – that the derived shapes are in some sense 'ideal' functional forms for dividing tough foods.

CONCLUSIONS

This analysis does not merely predict that points and blades will be present in dentitions designed for fracturing tough foods, as earlier studies have largely done (e.g. Lucas & Luke, 1984); it extends the examination to predict the detailed form in which the entire functional tooth will be found (including shape of blade edge and surface surrounding blades and points). The models presented above appear to be the best to date in terms of predictive power and resemblance with tooth shapes that occur in mammals.

This paper also demonstrates the potency of the approach of Maynard Smith *et al*. (1985) for identifying constraints in morphology, which involves the use of a priori knowledge of function to generate ideal forms along with evidence from convergence and maintenance of morphology throughout evolution. The method could be used much more frequently to detect the presence of constraints, and the proper identification of 'spandrels' (Gould & Lewontin, 1979; Pigliucci & Kaplan, 2000), in biological form.

Tooth modelling equips us with a method of simplifying and classifying the great diversity of tooth forms, such as variations of the basic carnassial or protoconoid forms. The evolution and degree of development of many features, such as single- or double-crested tooth shapes and the extent to which they conform to the functional criteria, may be tracked in fossil lineages, showing functional evolution of teeth in a new way. The possible paths of evolution can also be examined: for instance, there is only a limited number of basic arrangements of protoconoids possible, which will constrain the evolution of teeth even further.

This survey of tool morphospace confirms that there are only a limited number of shapes that conform to an 'ideal' functional morphology for teeth. This is also reflected in the high degree of conservation of many tooth forms. The causes are apparent: the limited options available in physics (in terms of function) and geometry (shape).

ACKNOWLEDGEMENTS

Our thanks go to Gudrun Arnold, Deb Archer, Martin Burd, Nuvan Aranwela, Mikael Fortelius, Alan Lill, Ralph Mac Nally, Jukka Jernvall and Betsy Dumont for comments on the concepts presented here and earlier drafts of this paper, and John Rensberger and an anonymous reviewer for helpful and insightful advice.

SUPPLEMENTARY MATERIAL

Full VRML reconstructions of all models constructed in this paper, from which Figures 2–4 have been drawn, are available from http://www.blackwell-publishing.com/products/journals/suppmat/BIJ/BIJ146/BIJ146sm.htm.

REFERENCES

Abler WL. 1992. The serrated teeth of tyrannosaurid dinosaurs and biting structures in other animals. *Paleobiology* **18:** 161–183.

Atkins AG, Vincent JFV. 1984. An instrumented microtome for improved histological sections and the measurement of fracture toughness. *Journal of Materials Science Letters* **3:** 310–312.

Butler PM. 1946. The evolution of carnassial dentitions in the Mammalia. *Proceedings of the Zoological Society of London* **116:** 198–220.

Crompton AW. 1971. The origin of the tribosphenic molar. In: Kermack DM, Kermack KA, eds. *Early mammals*. London: Academic Press, 65–87.

Crompton AW, Sita-Lumsden A. 1970. Functional significance of the therian molar pattern. *Nature* **227:** 197–199.

Cubberly WH, ed. 1989. *Tool and manufacturing engineers handbook*. Dearborn, MI: Society of Manufacturing Engineers.

Evans AR. 2000. Applications of confocal microscopy to functional morphology: the effect of diet and wear on tooth sharpness and function in two microchiropterans *Chalinolobus gouldii* and *C. morio*. Abstracts of the 9th Australasian Bat Conference, Tocal, Australia, 25–28 April 2001. *Bat Research News* **41:** 44.

Evans AR. in press. Quantifying the relationship between form and function and the geometry of the wear process in bat molars. In: Akbar Z, McCracken GF, Kunz TH, eds. *Functional and evolutionary ecology of bats: Proceedings of the 12th International Bat Research Conference*. New York: Oxford University Press.

Evans AR, Harper IS, Sanson GD. 2001. Confocal imaging, visualization and 3-D surface measurement of small mammalian teeth. *Journal of Microscopy* **204:** 108–118.

Evans AR, Sanson GD. 1998. The effect of tooth shape on the breakdown of insects. *Journal of Zoology* **246:** 391–400.

Frazzetta TH. 1988. The mechanics of cutting and the form of shark teeth (Chondrichthyes, Elasmobranchii). *Zoomorphology* **108:** 93–107.

Freeman PW. 1979. Specialized insectivory: beetle-eating and moth-eating molossid bats. *Journal of Mammalogy* **60:** 467–479.

Freeman PW. 1981. A multivariate study of the family Molossidae (Mammalia, Chiroptera): morphology, ecology, evolution. *Fieldiana Zoology* **7:** 1–173.

Freeman PW. 1992. Canine teeth of bats (Microchiroptera): size, shape and role in crack propagation. *Biological Journal of the Linnean Society* **45:** 97–115.

Freeman PW, Weins WN. 1997. Puncturing ability of bat canine teeth: the tip. In: Yates TL, Gannon WL, Wilson DE, eds. *Life among the Muses: Papers in honor of James S Findley*. Albuquerque, NM: The Museum of Southwestern Biology, 225–232.

Gould SJ. 1989. A developmental constraint in *Cerion*, with comments on the definition and interpretation of constraint in evolution. *Evolution* **43:** 516–539.

Gould SJ, Lewontin RC. 1979. The spandrels of San Marco and the Panglossian paradigm: a critique of the adaptationist programme. *Proceedings of the Royal Society of London, Series B* **205:** 581–598.

Knowles JR, Albery WJ. 1977. Perfection in enzyme catalysis: the energetics of triosephosphate isomerase. *Accounts of Chemical Research* **10:** 105–111.

Lessa EP, Stein BR. 1992. Morphological constraints in the digging apparatus of pocket gophers (Mammalia: Geomyidae). *Biological Journal of the Linnean Society* **47:** 439–453.

Lucas PW. 1979. The dental-dietary adaptations of mammals. *Neues Jahrbuch für Geologie und Paläontologie, Monatshefte* **1979:** 486–512.

Lucas PW. 1982. Basic principles of tooth design. In: Kurtén B, ed. *Teeth: form, function and evolution*. New York: Columbia University Press, 154–162.

Lucas PW, Luke DA. 1983. Methods for analysing the breakdown of food in human mastication. *Archives of Oral Biology* **28:** 813–819.

Lucas PW, Luke DA. 1984. Chewing it over: basic principles of food breakdown. In: Chivers DJ, Wood BA, Bilsborough A, eds. *Food acquisition and processing in primates*. New York: Plenum Press, 283–301.

Maynard Smith J, Burian R, Kauffman S, Alberch P, Campbell J, Goodwin B, Lande R, Raup D, Wolpert L. 1985. Developmental constraints and evolution. *Quarterly Review of Biology* **60:** 265–287.

Mellett JS. 1981. Mammalian carnassial function and the 'Every effect'. *Journal of Mammalogy* **62:** 164–166.

Mills JRE. 1966. The functional occlusion of the teeth of Insectivora. *Journal of the Linnean Society (Zoology)* **46:** 1–25.

Nee JG. 1998. *Fundamentals of tool design*. Dearborn, MI: Society of Manufacturing Engineers.

Osborn JW, Lumsden AGS. 1978. An alternative to 'thegosis' and a re-examination of the ways in which mammalian molars work. *Neues Jahrbuch für Geologie und Paläontologie Abhandlungen* **156:** 371–392.

Ostwald PF, Muñoz J. 1997. *Manufacturing processes and systems*. New York: John Wiley & Sons.

Pigliucci M, Kaplan J. 2000. The fall and rise of Dr Pangloss: adaptationism and the *Spandrels* paper 20 years later. *Trends in Ecology and Evolution* **15:** 66–70.

Pollack HW. 1976. *Tool design*. Reston, VA: Reston Publishing Co., Inc.

Popowics TE, Fortelius M. 1997. On the cutting edge: tooth blade sharpness in herbivorous and faunivorous mammals. *Annales Zoologici Fennici* **34:** 73–88.

Popowics TE, Rensberger JM, Herring SW. 2001. The fracture behaviour of human and pig molar cusps. *Archives of Oral Biology* **46:** 1–12.

Rensberger JM. 1973. An occlusal model for mastication and dental wear in herbivorous mammals. *Journal of Paleontology* **47:** 515–528.

Rensberger JM. 1995. Determination of stresses in mammalian dental enamel and their relevance to the interpretation of feeding behaviours in extinct taxa. In: Thomason JJ, ed. *Functional morphology in vertebrate paleontology*. Cambridge: Cambridge University Press, 151–172.

Sanson GD. 1980. The morphology and occlusion of the molariform cheek teeth in some Macropodinae (Marsupialia: Macropodidae). *Australian Journal of Zoology* **28:** 341–365.

Savage RJG. 1977. Evolution in carnivorous mammals. *Palaeontology* **20:** 237–271.

Seligsohn D. 1977. Analysis of species-specific molar adaptations in strepsirhine primates. In: Szalay FS, ed. *Contributions to primatology*, Vol. 11. Basel: S. Karger.

Sigogneau-Russell D, Hooker JJ, Ensom PC. 2001. The oldest tribosphenic mammal from Laurasia (Purbeck Limestone Group, Berriasian, Cretaceous, UK) and its bearing on the 'dual origin' of Tribosphenida. *Comptes Rendus de L'Academie des Sciences, Serie II, Sciences de la Terre et des Planètes* **333:** 141–147.

Silva M, Downing JA. 1995. *CRC handbook of mammalian body masses*. Boca Raton, LA: CRC Press.

Spears IR, Crompton RH. 1996. The mechanical significance of the occlusal geometry of great ape molars in food breakdown. *Journal of Human Evolution* **31:** 517–535.

Spears IR, Macho GA. 1998. Biomechanical behaviour of modern human molars: implications for interpreting the fossil record. *American Journal of Physical Anthropology* **106:** 467–482.

Stevens PS. 1974. *Patterns in nature*. Boston, MA: Atlantic Monthly Press.

Strait SG, Vincent JFV. 1998. Primate faunivores: physical properties of prey items. *International Journal of Primatology* **19:** 867–878.

Thompson D'AW. 1942. *On growth and form*. Cambridge: Cambridge University Press.

Van Valen L. 1966. Deltatheridia, a new order of mammals. *Bulletin of the American Museum of Natural History* **132:** 1–126.

Van Valkenburgh B. 1996. Feeding behavior in free-ranging large African carnivores. *Journal of Mammalogy* **77:** 240–254.

Worley M, Sanson G. 2000. The effect of tooth wear on grass fracture in grazing kangaroos. In: Spatz H-C, Speck T, eds. *Proceedings of the Plant Biomechanics Meeting.* Freiburg-Badenweiler: Georg Thieme, 583–589.

APPENDICES

These appendices contain instructions for generating the three-dimensional models of two ideal forms derived in this paper. Each file includes the 3-D coordinates for each corner of the shape (under the 'point' command) and the corners used to construct each face of the shape ('coordIndex'). The vectors of movement of the models are also given under the 'keyValue' of the 'PositionInterpolator' command. The code is entered in a simple text file with a .wrl extension. The file can be viewed using a VRML browser such as CosmoPlayer 2.1 for Windows (Computer Associates International, Inc., USA), available from http://www.ca.com/cosmo/. VRML browsers for Macintosh include Cortona VRML Client 1.1 (http://www.parallelgraphics.com/products/cortonamac/) and WorldView 2.0 (http://www.tucows.com/). CosmoPlayer and Cortona are plug-ins for web browsers (e.g. Netscape or Internet Explorer). Further instructions for viewing VRML files are given in Evans *et al.* (2001) and the Supplementary Material. VRML files for all models illustrated in this paper are available from A. Evans and in the Supplementary Material.

APPENDIX 1

VRML code for single-bladed tool with serial arrangement and lateral movement, as shown in Figure 4i.

```
# VRML V2.0 utf8
# VRML model of single-bladed tool
# with serial arrangement and lateral movement
#
# Alistair Evans & Gordon Sanson, 2002,
# Monash University
# alistair.evans@sci.monash.edu.au
WorldInfo {}
NavigationInfo {
 type ["EXAMINE", "WALK"] }
Background { skyColor 1 1 1 }

Transform {
 translation 14 0–10
 rotation 0 1 0 4
 children [
  DirectionalLight {
   direction 0 0 1
   ambientIntensity 1 }] }
Viewpoint {
 description "View A"
 position 2.32 2.26 –2.39
 orientation –0.07 0.97 0.23 2.51 }
Viewpoint {
 description "View B"
 position –2.87 2.39 –2.85
 orientation 0.08 0.98 0.18 3.95 }
Viewpoint {
 description "View C"
 position 0.33 1.31 5.55
 orientation 0.98 0.20 0.02 6.09 }

Transform {
 children [
  DEF LowerTool Shape {
   geometry IndexedFaceSet {
    solid FALSE
    coordIndex [
     0, 1, 2, 3, –1,
     0, 1, 5, 4, –1,
     1, 2, 6, 9, 5, –1,
     2, 3, 7, 6, –1,
     0, 8, 4, –1,
     3, 7, 8, –1,
     4, 5, 9, 8, –1,
     6, 7, 8, 9, –1]
    coord Coordinate {
     point [
      0 0 0,
      1 0 0,
      1 0 1,
      0 0 1,
      0 0.4 0,
      0.8 1 0,
      0.8 1 1,
      0 0.4 1,
      0 0 0.5,
      1 0.6 0.5] } }
   appearance DEF Appear Appearance {
    material Material {
     diffuseColor 1 1 1 } } } ] }

Transform {
 translation 0 0 1
 children [USE LowerTool] }

DEF TopTrans Transform {
 translation 1.68 1.84 0
 rotation 0 0 1 3.14159
 children [
```

```
  Transform {
   rotation 0 1 0 0
   children [
    DEF UpperTool Shape {
     geometry IndexedFaceSet {
      solid FALSE
      coordIndex [
       0, 1, 2, 3, –1,
       0, 1, 5, 4, –1,
       1, 2, 6, 9, 5, –1,
       2, 3, 7, 6, –1,
       0, 8, 4, –1,
       3, 7, 8, –1,
       4, 5, 9, 8, –1,
       6, 7, 8, 9, –1]
      coord Coordinate {
       point [
        0  0 0,
        1  0 0,
        1  0 1,
        0  0 1,
        0  0.4 0,
        0.8 1 0,
        0.8 1 1,
        0  0.4 1,
        0  0 0.5,
        1  0.6 0.5] } }
     appearance USE Appear } ] }
   Transform {
    translation 0 0 1
    rotation 0 1 0 0
    children [USE UpperTool] } ] }

DEF TS TimeSensor {
 loop TRUE
 cycleInterval 4 }

DEF TopMovePI PositionInterpolator {
 keyValue [
   1.56 2.08 0,
   2.04 1.12 0,
   1.56 2.08 0]
 key [0, 0.5, 1] }

ROUTE TopMovePI.value_changed TO TopTrans.
translation
ROUTE TS.fraction_changed TO TopMovePI.set_
fraction
```

APPENDIX 2

VRML code for double-bladed tool with serial arrangement and lateral movement, as shown in Figure 4ii.

```
#VRML V2.0 utf8
# VRML model of double-bladed tool
# with serial arrangement and lateral movement
#
# Alistair Evans & Gordon Sanson, 2002,
# Monash University
# alistair.evans@sci.monash.edu.au

WorldInfo {}
NavigationInfo {
 type ["EXAMINE", "WALK"] }
Background { skyColor 1 1 1 }

Transform {
 translation 14 0 –10
 rotation 0 1 0 4
 children [
DirectionalLight {
    direction 0 0 1
    ambientIntensity 1 } ] }
Viewpoint {
 description "View A"
 position 5.02 2.99 –3.84
 orientation –0.07 0.99 0.15 2.32 }
Viewpoint {
 description "View B"
 position –0.88 2.65 –5.27
 orientation 0 1 0.10 3.30 }
Viewpoint {
 description "View C"
 position –5.48 1.34 –0.73
 orientation 0.02 1 0.03 4.52 }

Transform {
 children [
  DEF Proto1 Shape {
   geometry IndexedFaceSet {
    solid FALSE
    coordIndex [
     0, 1, 2, –1,
     0, 1, 4, 8, 3, –1,
     0, 2, 10, 6, 3, –1,
     1, 2, 10, 7, 4, –1,
     5, 6, 10, –1,
     5, 7, 10, –1,
     5, 6, 7, –1,
     6, 7, 9, –1,
     3, 6, 9, 8, –1,
     4, 7, 9, 8, –1]
    coord Coordinate {
     point [
      0.1 0 0,
      0.9 0 0,
      0.5 0 0.693,
      0 1.2 0,
      1 1.2 0,
      0.5 2 0.433,
      0.25 1.3 0.433,
      0.75 1.3 0.433,
      0.5 0.8 0,
      0.5054 1.1114 0.3163,
      0.5 1.3 0.866] } }
   appearance DEF Appear Appearance {
    material Material {
     diffuseColor 1 1 1 } } } ] }

DEF Transform Transform {
 translation –1 0 0
 children [USE Proto1] }

DEF TS TimeSensor {
 loop TRUE
 cycleInterval 4 }
```

```
DEF TopTrans Transform {
 translation 0.5 3.08 0.519
 rotation 0 1 0 0
 children [
  DEF Transform_2 Transform {
   rotation 1 0 0 3.141
   children [USE Proto1] }
  DEF Transform_3 Transform {
   translation –1 0 0
   rotation 1 0 0 3.141
   children [USE Proto1] } ] }
```

```
DEF TopMovePI PositionInterpolator {
 keyValue [
  0.5 3.26 0.39,
  0.5 2.54 0.909,
  0.5 3.26 0.39]
 key [0, 0.5, 1] }

ROUTE TS.fraction_changed TO TopMovePI.set_
fraction
ROUTE TopMovePI.value_changed TO TopTrans.
translation
```